

# Ultrasound thermometry in transparent and opaque fluids

S. Fife, C.D. Andereck, S. Rahal

152

**Abstract** We have exploited the temperature dependence of sound velocity to measure the thermal fields in transparent and opaque fluids. A chamber containing glycerol undergoing Rayleigh–Bénard convection was probed with an ultrasound transducer operating in the pulse-echo mode. The times-of-flight for the ultrasound pulse to traverse the fluid at several transducer locations were converted into a temperature profile that is in qualitative agreement with simultaneous thermochromic liquid crystal visualization of the flow pattern. Temperature profiles in a mercury-filled stainless steel chamber have also been obtained, both for quiescent and turbulent flows, thereby validating the ultrasound thermometry concept for opaque fluids as well.

## 1 Introduction

The study of natural convection of fluids driven by temperature gradients has a long and rich history. Bénard (or Marangoni) convection, in which surface tension at a free upper boundary plays a dominant role, was one of the first such systems studied in any detail. The buoyancy driven flows of fluids in systems with rigid boundaries at the top and bottom (Rayleigh–Bénard convection) have been extensively studied, both for their potential applications and as beautiful examples of pattern formation in non-equilibrium systems (for reviews of convection in single layers and related pattern forming systems, see Cross and Hohenberg 1993; Koschmieder 1993 and Bodenschatz et al. 2000). Partially as a result of having a large variety of diagnostic tools that can be brought to bear, most convection experiments have been performed with transpar-

ent fluids. However, the importance of studying the thermally driven flows of opaque fluids, such as liquid metals, some viscoelastic polymer melts and solutions, and ferrofluids, cannot be minimized: They are interesting from a fundamental fluid dynamics perspective since their thermal (and/or mechanical) properties are often quite different from typically used transparent Newtonian fluids. Furthermore, they are important in many industrial processes. (A particular example of the latter would be semiconductor crystal growth dynamics in a Bridgman apparatus. Destructive testing of the crystal after the process is complete gives only indirect information about the fluid dynamics of the formation process. Knowledge of the thermal and velocity fields during the growth process is essential.) Attempts to mimic the flow behaviors of such fluids under thermal stress using the normally employed oils or water are likely to fail (see, for example, Carpenter and Homay 1989), who discuss the large effect of the Prandtl number on surface tension gradients), so ways must be found to deal with the actual fluids in question. Therefore, innovative measurement techniques applicable to a variety of opaque fluids are desirable, both for use in fundamental flow studies and in applications. In this paper we describe one solution to this problem.

## 2 Review of existing techniques

Before describing our approach, it will be helpful to briefly review the various diagnostic tools currently available. Relatively non-intrusive velocity and temperature measurements in fluids typically rely on optical techniques, and hence are useful only with transparent fluids. For example, laser Doppler velocimetry (LDV) and particle imaging velocimetry (PIV) rely on the addition to the flow of small seed particles to determine the velocity field (see, for example, Somerscales 1981; Jacobs et al. 1988; Guezennec et al. 1994). A very different type of approach is to use the variation of the index of refraction of the fluid with temperature to visualize the thermal field through interferometric, schlieren, or shadowgraph techniques (Goldstein 1983; Prakash and Koster 1996; Settles 2001). In each case the result is a 2D map related to the average of the temperature field along the line of observation.

For opaque fluids very different measurement approaches are necessary. To determine local temperatures, one may insert thermistors or thermocouples directly into the flow, or embed them in the chamber walls. Unfortunately, the former method is quite intrusive and the latter does not yield data from the interior of the flow. Similarly,

---

Received: 22 August 2002 / Accepted: 2 April 2003  
Published online: 28 June 2003  
© Springer-Verlag 2003

S. Fife, C.D. Andereck (✉)  
Department of Physics,  
The Ohio State University, Columbus, OH43210, USA  
E-mail: Andereck.1@osu.edu

S. Rahal  
Department of Mechanical Engineering,  
University of Batna, Batna, Algeria

The authors wish to thank NASA for its generous support through grant NAG3-2138. We also wish to thank S.I. Rokhlin, M. Rutgers, Y. Takeda, and P. Tong for helpful discussions and useful insights.

hot-wire or hot-film probes may be used to make local velocity measurements (Blackwelder 1981). Unfortunately, these probes can also be quite invasive. Furthermore, it is not easy to scan the flow field, since the probe is either wall-mounted or is suspended by a small boom that must pass through a wall of the system (in the case of an enclosed flow). A recent development is the ultrasound Doppler velocimeter (Takeda 1986; Takeda 1987; Takeda 1991). As in its optical counterpart, it relies on seed particles to scatter Doppler shifted sound back to the detector. In contrast with the optical case, Doppler ultrasound works in both transparent and opaque fluids. Commercial units of this sort can detect velocities as low as a few cm/s, which limits the usefulness of the technique in weak flows or with delicate patterns such as might be found near the onset of convection. In addition, Doppler ultrasound techniques may not be appropriate for studying convective fluid flow in crystal growth because particle seeding is unacceptable and flow velocities are usually very low. The velocities can be vanishingly small in microgravity conditions where buoyancy is negligible, whereas temperature gradients may still be quite large.

It is also possible to use X-rays in a manner similar to the use of visible light in the optical techniques described previously. Signal attenuation differences caused by sample density variations and discontinuities underlie medical imaging and non-destructive testing of solids. This approach has been used for imaging density variations in solidification and convection (Campbell and Koster 1994; Pool and Koster 1994; Campbell and Koster 1995a; Campbell and Koster 1995b; Koster 1997; Koster et al. 1997a; Koster et al. 1997b; and Derebail and Koster 1998). There are drawbacks. Radiological methods require care to ensure safety, but this is not an insurmountable problem. Producing energetic X-rays requires considerable power input, which is a potential problem in space-based experiments. More importantly there are limitations on the depth of the fluid that may be probed, at least for liquid metals: The penetration depth for X-rays is a fraction of a cm for energies up to 1 MeV for mercury (Koster 1997). As a result, the experiments referenced above were for test cells of only a few mm thickness. Although X-ray densitometry has proven to be a valuable diagnostic tool in certain situations involving opaque fluids, there are limitations on its general usefulness.

Very recently ultrasound scattered from impurities in solid samples has been used to map thermal fields (Seip et al. 1996; Simon et al. 1997; Simon et al. 1998; Le Floch et al. 1999). Extension of this technique to fluids would again require seeding.

In summary, although a variety of techniques exist for the measurement of velocity and temperature fields, none are entirely satisfactory if we are interested in studying, non-invasively, the flow of opaque fluids.

### 3 Ultrasound thermometry

We have used ultrasound to detect the thermal field of a liquid metal non-intrusively and without the use of seed particles. The technique relies upon the variation of sound speed with the temperature of the fluid. The use of sound

speed to measure the temperature of a gas was apparently first proposed by Mayer (1873). More recently the concept has been realized in large-scale gas systems (such as in the interiors of furnaces and boilers) by Morgan (1972), Dadd (1983), Green (1985), Bramanti et al. (1996), and Sielschott (1997). To apply the concept to small-scale liquid-filled chambers we have adopted the pulse-echo ultrasound technique commonly employed for non-destructive testing of solids (Birks and Green 1991). Specifically, a very short ultrasound pulse traverses the chamber in a time determined by the chamber geometry and the average temperature of the fluid through which it passes. Our goal is to measure the time between the arrival of an echo pulse from the first wall/liquid interface and the arrival of a pulse from the second such interface, on the far side of the chamber. Owing to the size of the systems we work with, and the relatively small variation of the liquid's sound speed with temperature, the measurement demands are stringent. (For perspective, the temperature dependence of sound velocity in liquid metals is comparable to the temperature dependence of the index of refraction required for accurate interferometric thermal images in transparent fluids.) Nevertheless, with high-speed instrumentation we can detect the influence of the fluid temperature on the pulse travel time and thus obtain temperature measurements of the fluid interior. With the present system, spatial resolution of a few millimeters or less is achievable with moderate transducer resonant frequencies (the wavelength is  $\sim 0.04$  cm for mercury, for instance). Temperature resolution of a fraction of a degree Celsius has been achieved. With an array of transducers scanned electronically a map of the thermal field over the chamber can be produced on a time scale short compared with many convective processes. While we cannot yet achieve the speed or resolution of optical systems, ultrasound thermometry is nonetheless quite adequate for many flow problems.

There are some potential difficulties with the technique. First, the approach we take in extracting temperature profiles from the data involves a simplification of the actual situation, but a justifiable one. One simplifying notion is that the ultrasound beam is a plane wave with no divergence. In fact, the sound field of a transducer is quite complex, particularly in the near field (Birks and Green 1991). However, in the case of a pulse signal we can distinguish between echoes that have reflected from the far wall and those that come from other directions, as the latter must occur at a later time and will be of considerably smaller amplitude. A second approximation is that the beam propagates in a straight line, when in fact there will be some deflection caused by temperature gradients transverse to the beam. This is a small effect and quite negligible for the sorts of temperature gradients we are measuring. Even for the thermal field in a furnace, with temperature variations of hundreds of degrees Kelvin, the estimated error caused by this effect is 2% or less (Green 1985). Another potential source of error is a Doppler shift owing to fluid velocity along the line of sight. The flows we have studied have small or vanishing components along the line of sight. In any event, if there is such a component the fact that the ultrasound pulses traverse the fluid both with and against that component would cancel to first

order any effect caused by that velocity component. In sum, for the kinds of measurements we are undertaking, the simplest approximation is quite adequate and is justified by our results.

#### 4 Experimental apparatus

Two distinct configurations were used in these exploratory investigations. In initial work with glycerol as the con-  
ducting fluid, a single ultrasound transducer was mounted on a system of manually controlled translation stages. A small spring presses the transducer against the chamber wall. Acoustic coupling to the system was aided by a thin layer of glycerol between the transducer and the chamber wall. Glycerol was chosen (coincidentally) as the working fluid for compatibility with encapsulated thermochromic liquid crystal particles that we introduced for visualization purposes. The transducer was a model M110 from Panametrics (Waltham, Mass., USA), which has a 5.0 MHz resonant frequency and 6 mm diameter. The transducer was driven by a Panametrics model 5800 pulser/receiver, which sends a high-voltage pulse to the transducer and then receives the resulting signal. The output signal was in turn detected by a TDS 580D 1 GHz digital oscilloscope (Tektronix, Inc., Beaverton, Oreg., USA), which operated in an averaging mode (typically 256 pulses) to increase the signal-to-noise ratio. This apparatus is shown schematically in Fig. 1. Example signals and details are shown in Figs. 2 and 3.

The experimental procedure for the single transducer configuration was as follows. Calibration was achieved by measuring the transit time across the chamber as a function of temperature, with no vertical temperature gradients (and thus no convection) present. The system was brought to the initial desired temperature and allowed to reach a steady state over a period of approximately an hour. The ultrasound transit time was obtained by time shifting of the second echo with respect to the first using an internal function of the oscilloscope. The fluid temperature was then slowly changed to a new value and the transit time was determined again. A calibration graph such as Fig. 4 resulted. The solid lines are linear fits that can then be used for interpreting subsequent measurements when there is a temperature gradient in the fluid. In this early work a horizontal scan of the system was performed, but only at the initial temperature. The variations in width of the chamber as determined by this scan were then used to correct the raw measurements obtained later.

We also constructed a transducer array consisting of five identical transducers uniformly spaced along a line (see Fig. 5). The center-to-center spacing was  $\sim 9.75$  mm. The transducers were separately spring loaded. The array was connected to a model 7002 switcher (Keithley Instruments, Inc., Cleveland, Oh., USA), which, under computer control, can shift the electrical connection to the Panametrics pulser/receiver from one transducer to the next with approximately 0.15 s dead time. The output of the pulser/receiver is sent to a preamplifier, which allows us to adjust the voltage offset and gain so that the signal excursions are maximized within the input range of the Eclipse (Signal Recovery, Oak Ridge, Tenn., USA), a very

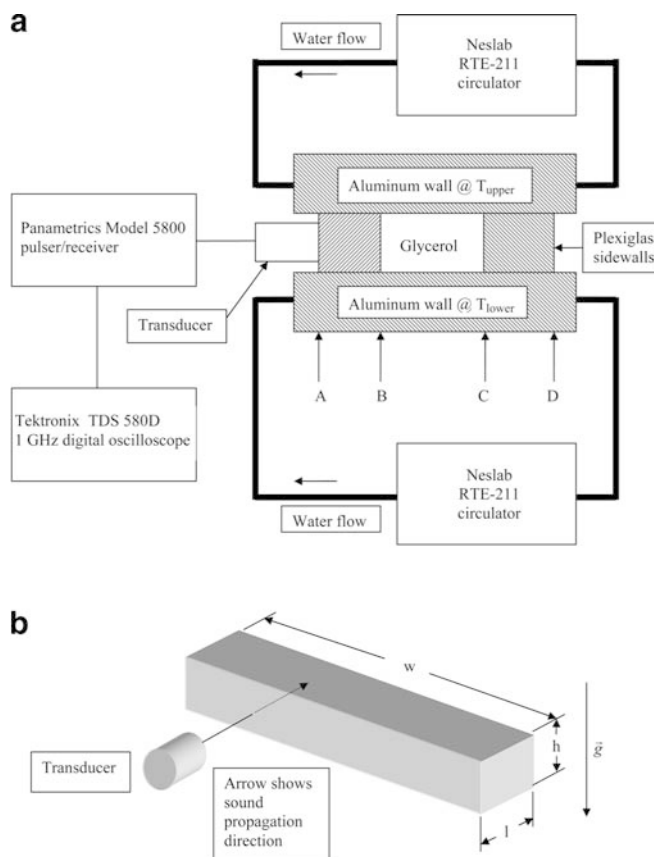


Fig. 1. **a** Schematic diagram of the glycerol-filled convection cell, the circulating bath temperature controllers, a movable ultrasound transducer, and the associated electronics for acquiring and analyzing the signal from the transducer. Locations A–D refer to Fig. 2. **b** Dimensions of the fluid-filled cavity:  $l$  is 2 cm,  $w$  is 7.8 cm, and  $h$  is 1.2 cm. The transducer and the directions of sound propagation and of gravity are included for reference

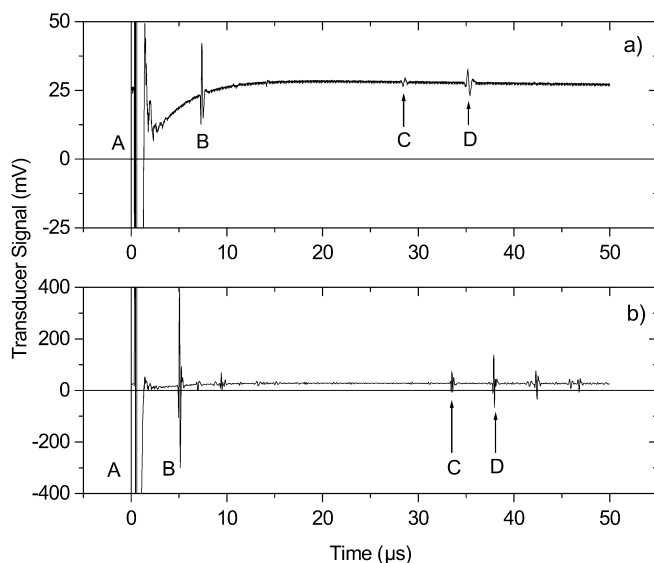


Fig. 2. Typical transducer signals for a glycerol in acrylic plastic and **b** mercury in stainless steel. The letter A corresponds to the initial pulse plus whatever echo returns from interface A in Fig. 1, hidden in the very large (and outside of range) initial signal. The remaining letters correspond to the other interfaces in Fig. 1. The time between echos B and C ( $\delta t$  in Fig. 4) represents twice the transit time to cross the chamber once

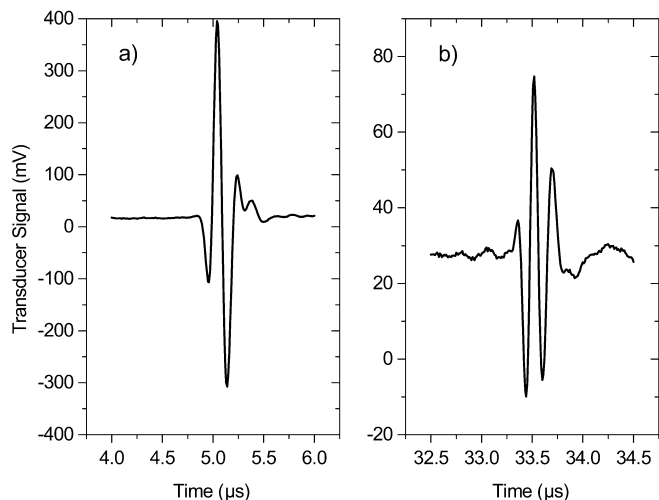


Fig. 3. Enlargements of a echo B and b echo C, from Fig. 2b, a signal for mercury in stainless steel, showing the very narrow peak widths ( $\sim 0.1 \mu\text{s}$ ) and the rapid damping of the pulse

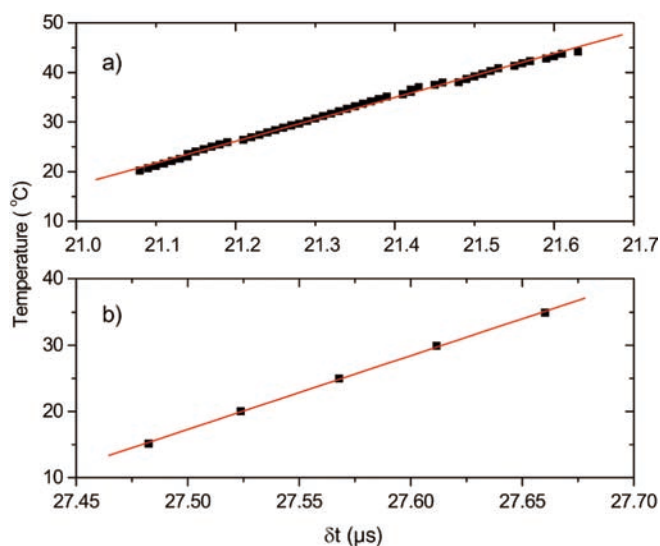


Fig. 4. Typical calibration curves for a glycerol in acrylic plastic and b mercury in stainless steel.  $\delta t$  is twice the transit time through the fluid. The fit function for glycerol is  $T = -910.979 C + (44.203 C/\mu\text{s})\delta t$  and for mercury it is  $T = -3049.0 C + (111.5 C/\mu\text{s})\delta t$

high-speed signal averager. In the Eclipse, signals from a particular transducer accumulate until an averaged output can be transferred to the computer, and the switcher brings the next transducer online. The LabView program (National Instruments Corp., Austin, Tex., USA) responsible for control of the data acquisition then finds the appropriate peaks in the averaged signal and stores their locations for additional processing after the data run is completed. It is possible to obtain a complete scan of the array, with 1024 pulses per transducer, in  $\sim 7.6$  s. This is a great improvement over manually translating a single transducer from location to location, which under optimal conditions can take 40 s per position shift. Following initial processing of the data, a background file is used to remove the effect of the static shape non-uniformities of

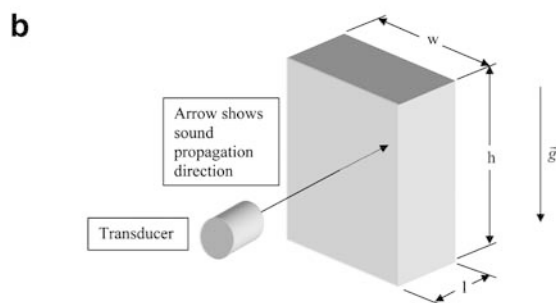
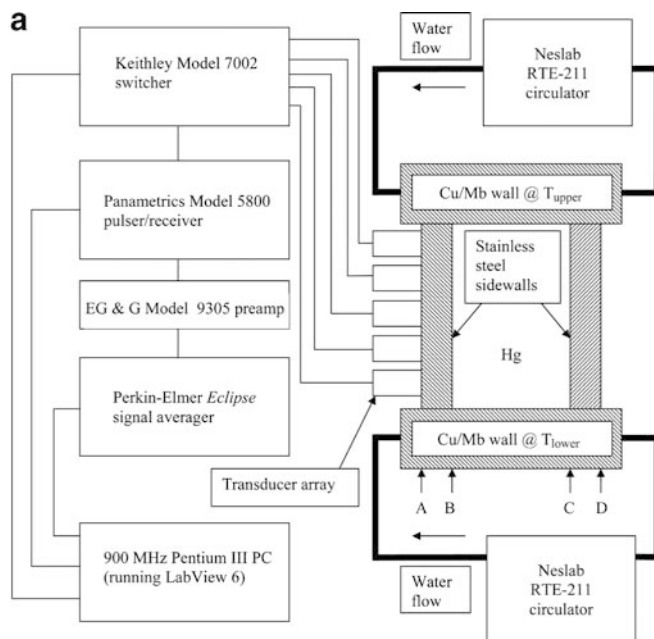


Fig. 5. a Schematic diagram of the mercury-filled experimental cell and the circulating bath temperature controllers, a five-transducer array, and associated electronics. b Dimensions of the fluid-filled cavity:  $l$  is 2.0 cm,  $w$  is 3.8 cm, and  $h$  is 5.0 cm. A transducer, the direction of sound propagation and the direction of gravity are included for orientation

the chamber, leaving transit times that reflect the fluid thermal profile.

## 5 Initial results

Proof-of-concept experiments with a single transducer and oscilloscope were conducted in a glycerol-filled chamber constructed with acrylic plastic sidewalls and aluminum top and bottom walls through which flowed water from RTE-211 circulating bath temperature controllers (Thermo Neslab, Austin, Tex., USA). The chamber was 1.30 cm high  $\times$  2.00 cm deep (along the ultrasound propagation direction, parallel to the convection roll axes)  $\times$  7.8 cm long. (Thermal and acoustic properties of all materials and fluids used are listed in Table 1. Note that acrylic plastic and glycerol have similar acoustic impedances, which makes it relatively easy to achieve transmission through interfaces between them (Shutilov 1988).) The walls through which the ultrasound propagated were 9.3 mm thick. A typical procedure would be to start with the top and bottom plates set to the same temperature, approximately that of the room. The bottom plate temperature

**Table 1.** Properties of materials used. All values for mercury and glycerol are for 20 C, except for the thermal conductivity of mercury, which is quoted for 25 C. The glycerol values are calculated using the temperature dependent formulas from Stengel et al. (1982)

Material	Property							
	Density $\rho$ ( $\times 10^3$ kg/m <sup>3</sup> )	Sound velocity $C$ (m/s)	Acoustic impedance $Z$ ( $\times 10^6$ )	Thermal conductivity $k$ (W/mK)	Prandtl number $Pr$	Volume thermal expansion coefficient $3\alpha$ ( $\times 10^{-6}$ )	Kinematic viscosity $\nu$ (cm <sup>2</sup> /s)	Thermal diffusivity $\kappa$ (cm <sup>2</sup> /s)
Stainless steel	7.85	5,790	45.0	14.4		33.0		
Molybdenum				138.0				
Acrylic glass	1.19	2,750	3.19	0.19		202.2		
Aluminum				237.0		69.0		
Mercury	13.55	1,450	19.66	8.25	0.025	181.0	0.00114	0.046
Glycerol	1.26	1,904	2.4	0.285	11,800	470.0	11.18	0.000946

then would be slowly increased over several hours, while the top plate temperature was simultaneously lowered. At the desired  $\Delta T$  the temperature ramping was halted and the system was allowed to reach a steady state, after which data acquisition would commence. Since the output was a time delay between first echo and second echo as determined by reading the oscilloscope manually, it typically took several minutes to complete a scan. Nonetheless, a convincing temperature profile could be extracted, as shown in Fig. 6 for a case of vertical  $\Delta T$  of 11.45 C, corresponding to a Rayleigh number based on the average temperature of the fluid of 3,282, or 1.92 times  $Ra_c$  (note that glycerol has highly temperature dependent thermal and mechanical parameters and in actuality the fluid is highly non-Boussinesq, to the point that it is not apparent that a single Rayleigh number properly characterizes the flow state (Stengel et al. 1982; Zhang et al. 1997)). The spatial dependence is apparent, with higher temperature regions corresponding to rising warm fluid and lower temperature regions corresponding to falling cool fluid.

To confirm this result we took advantage of the transparency of the fluid to introduce microencapsulated thermochromic liquid crystals (type R29C4 W, Hallcrest, Inc., Glenview, Ill., USA) into the flow. They were chosen for their sensitivity in the particular temperature range within which we worked. It is clear from Fig. 6 that well-defined convection rolls were present in the system, and that the warm and cool regions revealed by the liquid crystal color variations correspond with the temperature profile detected by the ultrasound measurements, thereby establishing the validity of the ultrasound thermometry concept in this application.

The ultimate aim of our work has been to develop a diagnostic tool for use in optically opaque fluids, possibly enclosed by walls that are also opaque. As an initial test of the concept we have performed some measurements on mercury in a stainless steel chamber using the five transducer array described previously and sketched in Fig. 5. The chamber had an inner height of 5.00 cm, a depth along the direction of ultrasound propagation of 2.00 cm, and a length of 3.8 cm. The sidewalls, made of stainless steel, were 8.3 mm thick. Again, the acoustic impedances of mercury and stainless steel (Table 1) are similar enough to allow for good transmission through interfaces between them. At the top and bottom of the chamber 2.5 mm thick molybdenum plates were in contact with the mercury, which were in turn backed by copper blocks through which flowed water from Neslab RTE-211 circulating bath temperature controllers. The molybdenum plate temperatures were monitored by thermistors (model P65DB103 J, Thermometrics, Edison, N.J., USA) embedded in them within  $\sim 2$  mm of the surface exposed to the mercury. To simplify the situation initially we measured the thermal profile under a stabilizing imposed temperature gradient (i.e., hotter at the top of the chamber than at the bottom). In this case we expected a simple linear temperature profile. Figure 7 shows the outcome for several different imposed temperature differences: for this situation, the data of interest form the three lines with positive slope in that graph. In all cases the profiles are as expected. If we project the linear fits to the ends of the chambers the overall temperature difference from the top to the bottom of the chamber as measured by the ultrasound technique is virtually identical to that given by the embedded

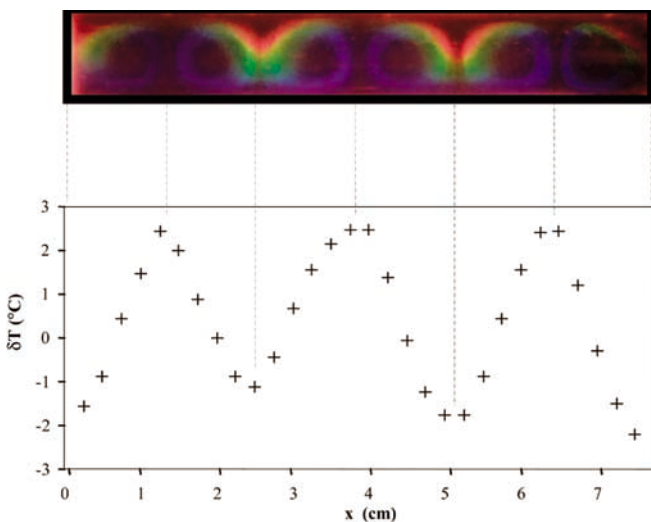


**Fig. 6.** Encapsulated liquid crystal (Hallcrest R29C4 W) seeded flow of glycerol at  $\Delta T=11.45$  C, showing the convection rolls. The red start is at  $\sim 29$  C, while blue begins at  $\sim 33$  C. Our particular sample was not calibrated. The plot shows the temperature profile measured using a movable single ultrasound transducer

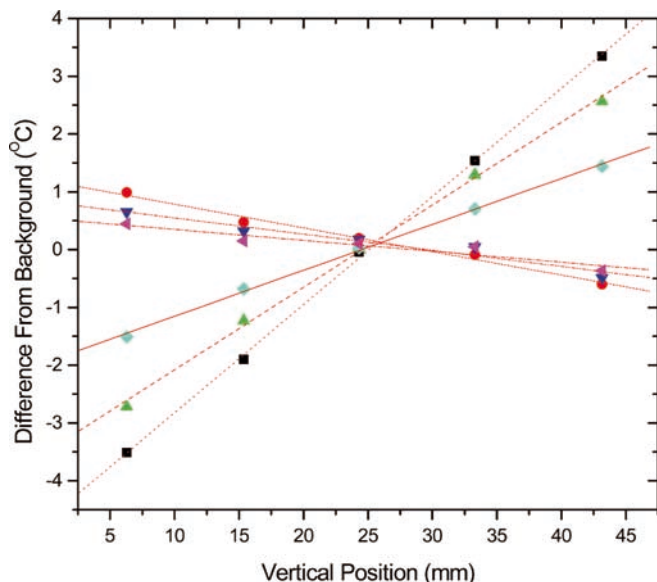


Fig. 7. Temperature profiles for heating from above (*solid square* 9.5 C; *solid triangle* 7.2 C; *solid diamond* 3.9 C) and heating from below (*solid circle* 9.5 C; *inverted solid triangle* 7.2 C; *left-pointing solid triangle* 3.9 C). Heating from below gives rise to turbulent convection. In that case, the temperature differences correspond to the following Rayleigh numbers: 9.5 C  $\rightarrow Ra=4.39 \times 10^6$ , 7.2 C  $\rightarrow Ra=3.33 \times 10^6$ , and 3.9 C  $\rightarrow Ra=1.80 \times 10^6$

thermistors. We conclude that ultrasound thermometry yields a quantitatively accurate measurement of the temperature profile.

A more stringent test of the capabilities of the system can be made by working with a fluid undergoing turbulent convection. We used the same mercury/stainless steel chamber combination as in the previous experiments and established turbulent convection at large  $\Delta T$  for temperature profile comparison with the case of no convection. For this purpose we adjusted the circulator temperatures to give the same magnitude imposed temperature difference, but hotter on the bottom plate than on the top, thus imposing a destabilizing gradient on the fluid. By imposing a sufficiently large gradient the convecting fluid was driven into turbulence, based on the very high Rayleigh numbers achieved in each run, and, in fact, time-series measurements with the array showed fluctuating temperatures. The time dependences observed for the two cases are shown in Fig. 8. While there are some fluctuations even in the stabilized case, presumably because of measurement error, they are larger in the case of turbulent convection in the mercury, clearly above the level of the measurement precision. The measured standard deviation for this transducer location is 0.16 C in the turbulent case and only 0.05 C in the quiescent case.

To extract a temperature profile from the turbulent flows we time-averaged the data from each transducer and plotted only the mean temperature against transducer location. The result is shown in Fig. 7 as the lines with small negative slope. The difference in magnitude of the slopes of the lines for the stable and turbulent cases is striking. For the stable case the slope is as expected, a simple linear temperature profile. In the case of turbulent

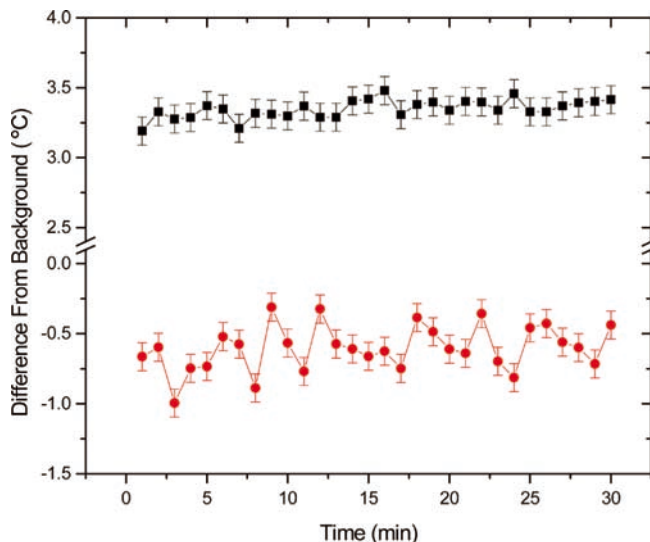


Fig. 8. Time traces from the uppermost transducer in Fig. 7, for no convection (*solid square* 9.5 C) and for turbulent convection (*solid circle* 9.5 C,  $Ra=4.39 \times 10^6$ ). The error bars represent the approximate measurement precision based on finding a peak using a built-in LabView routine

convection the absolute value of the slope is much lower over the core of the chamber, the region probed by the transducers. This is consistent with other experiments in the literature (Takeshita et al. 1996; Zhang et al. 1997), which show that for very large Rayleigh numbers the core of the flow is nearly isothermal, while the bulk of the temperature variation occurs in the thermal boundary layers at the top and bottom of the chamber. Our measurements using ultrasound thermometry are consistent with this observation, although the slopes are not vanishingly small as might have been expected. Of course, our technique gives only an average measurement across the chamber, and near the side walls one does not expect to see the same isothermal core profiles as in the interior.

## 6 Conclusions

We have shown that ultrasound thermometry is feasible for small-scale laboratory experiments on convection, including convection in a liquid metal. Our results have been validated by using the technique on a roll pattern in a transparent fluid where a conventional approach was also feasible. In addition, our results are consistent with the predicted behavior in the case of a liquid metal for both a simple conduction state (quiescent) and a turbulent flow. The temperature sensitivity varies depending upon the magnitude of the variation of the sound speed in each liquid, but for our cases we have achieved resolutions on the order of 0.1 C. The spatial resolution is on the order of the transducer diameter.

The next step in the development of this technique will be to modify the array to include more and smaller transducers. In addition we will add computer-controlled traversing mechanisms to allow for rapid 2D scans, scans that should yield images of the flow comparable to the shadowgraph images obtainable in transparent fluids.

Eventually it may be possible to produce localized thermal field measurements using tomographic reconstruction, as has already been done in large-scale gas systems (Green 1985). As the technique becomes more fully developed, it should prove a useful diagnostic in a variety of flow problems involving liquid metal convection with various boundary conditions, solidification studies, and other situations in which the usual diagnostics simply do not work or work in a very inconvenient or intrusive fashion.

## References

- Birks AS, Green RE (1991) *Nondestructive testing handbook*, vol 7. Ultrasonic testing. American Society for Nondestructive Testing, Columbus, Ohio
- Blackwelder RF (1981) Hot-wire and hot-film anemometers. In: Emrich RJ (ed) *Fluid dynamics, Part A: Methods of experimental physics*, vol 18. Academic Press, New York, pp 259–314
- Bodenschatz E, Pesch W, Ahlers G (2000) Recent developments in Rayleigh–Bénard convection. *Ann Rev Fluid Mech* 32:709–778
- Bramanti M, Salerno EA, Tonazzini A, Pasini S, Gray A (1996) An acoustic pyrometer system for tomographic thermal imaging in power plant boilers. *IEEE Trans Instrum Meas* 45:159–167
- Campbell TA, Koster JN (1994) Visualization of liquid–solid interface morphologies in gallium subject to natural convection. *J Cryst Growth* 140:414–425
- Campbell TA, Koster JN (1995a) A novel vertical Bridgman–Stockbarger crystal growth system with visualization capability. *Meas Sci Technol* 6:472–476
- Campbell TA, Koster JN (1995b) Radioscopic visualization of indium antimonide growth by the vertical Bridgman–Stockbarger technique. *J Cryst Growth* 147:408–410
- Carpenter BM, Homsy GM (1989) Combined buoyant-thermocapillary flow in a cavity. *J Fluid Mech* 207:121–132
- Cross MC, Hohenberg PE (1993) Pattern formation outside of equilibrium. *Rev Mod Phys* 65:851–1112
- Dadd MW (1983) Acoustic thermometry in gases using pulse techniques. Paper presented at the TEMCON Conference, London
- Derebail R, Koster JN (1998) Visualization study of melting and solidification in convecting hypoeutectic Ga–In alloy. *Int J Heat Mass Transfer* 41:2537–2548
- Goldstein RJ (1983) *Fluid mechanics measurements*. Washington: Hemisphere, Springer
- Green SF (1985) An acoustic technique for rapid temperature distribution measurement. *J Acoust Soc Am* 77:759–763
- Guezennec YG, Brodkey RS, Trigui N, Kent JC (1994) Algorithms for fully automated three-dimensional particle tracking velocimetry. *Exp Fluids* 17:209–219
- Jacobs DA, Jacobs CW, Andereck CD (1988) Biological scattering particles for laser Doppler velocimetry. *Phys Fluids* 31:3457–3461
- Koschmieder EL (1993) *Bénard cells and Taylor vortices*. Cambridge University Press, Cambridge
- Koster JN (1997) Visualization of Rayleigh–Bénard convection in liquid metals. *Europ J Mech B/Fluids* 16:447–454
- Koster JN, Derebail R, Grotzbach A (1997a) Visualization of convective solidification in a vertical layer of eutectic Ga–In melt. *Appl Phys A—Materials* 64:45–54
- Koster JN, Seidel T, Derebail R (1997b) A radioscopic technique to study convective fluid dynamics in opaque liquid metals. *J Fluid Mech* 343:29–41
- Le Floch C, Tanter M, Fink M (1999) Self-defocusing in ultrasonic hyperthermia: experiment and simulation. *Appl Phys Lett* 74:3062–3064
- Mayer AM (1873) On an acoustic pyrometer. *Phil Mag* 45:18–22
- Morgan ES (1972) The acoustic gas pyrometer. CEGB Report RD/L/R 1779
- Pool RE, Koster JN (1994) Visualization of density fields in liquid metals. *Int J Heat Mass Transfer* 37:2583–2587
- Prakash A, Koster JN (1996) Steady Rayleigh–Bénard convection in a two-layer system of immiscible liquids. *Trans Am Soc Mech Eng* 118:366–373
- Seip R, Vanbaren P, Cain CA, Ebbini ES (1996) Noninvasive real-time multipoint temperature control for ultrasound phased array treatments. *IEEE Trans Ultrason Ferroelect Freq Control* 43:1063–1073
- Settles GS (2001) *Schlieren and shadowgraph techniques*. Springer, Berlin Heidelberg New York
- Shutilov VA (1988) *Fundamental physics of ultrasound*. Gordon and Breach, New York
- Sielschott H (1997) Measurement of horizontal flow in a large scale furnace using acoustic vector tomography. *Flow Meas Instrum* 8:191–197
- Simon C, VanBaren P, Ebbini E (1997) Quantitative analysis and applications of non-invasive temperature estimation using diagnostic ultrasound. In Schneider SC, Levy M, McAvoy BR (eds) *Proceedings, IEEE Ultrasonics Symposium*, 5–8 October 1997. IEEE, New York, pp 1319–1322
- Simon C, Vanbaren P, Ebbini ES (1998) Two-dimensional temperature estimation using diagnostic ultrasound. *IEEE Trans Ultrason Ferroelect Freq Control* 45:1088–1099
- Somerscales EFC (1981) Tracer methods: laser Doppler velocimetry. In: Emrich RJ (ed.) *Fluid dynamics, Part A: Methods of experimental physics*, vol 18. Academic, New York, pp 93–240
- Stengel KC, Oliver DS, Booker JR (1982) Onset of convection in a variable-viscosity fluid. *J Fluid Mech* 120:411–431
- Takeda Y (1986) Velocity profile measurement by ultrasound Doppler shift method. *Int J Heat Fluid Flow* 7:313–318
- Takeda Y (1987) Measurement of velocity profile of mercury flow by ultrasound Doppler shift method. *Nucl Technol* 79:120–124
- Takeda Y (1991) Development of an ultrasound velocity profile monitor. *Nucl Eng Des* 126:277–284
- Takeshita T, Segawa T, Glazier JA, Sano M (1996) Thermal turbulence in mercury. *Phys Rev Lett* 76:1465–1468
- Zhang J, Childress S, Libchaber A (1997) Non-Boussinesq effect: thermal convection with broken symmetry. *Phys Fluids* 9:1034–1042